Two-dimensional spin-imbalanced Fermi gases at nonzero temperature: Phase separation of a noncondensate

Chien-Te Wu, Rufus Boyack, and K. Levin

Phys. Rev. A **94**, 033604 — Published 6 September 2016

DOI: 10.1103/PhysRevA.94.033604

Two-dimensional spin-imbalanced Fermi gases at non-zero temperature: Phase separation of a non-condensate

Chien-Te Wu, Rufus Boyack, and K. Levin
James Franck Institute, University of Chicago, Chicago, Illinois 60637, USA

We study a trapped two-dimensional (2D) spin-imbalanced Fermi gas over a range of temperatures. In the moderate temperature regime, associated with current experiments, we find reasonable semi-quantitative agreement with the measured density profiles as functions of varying spin imbalance and interaction strength. Our calculations show that, in contrast to the three-dimensional case, the phase separation which appears as a spin balanced core, can be associated with non-condensed fermion pairs. To shed light on the nature of 2D quasi-condensation we compute the momentum, q, distribution of pairs, called $n_B(\mathbf{q})$; a pronounced low momentum peak is found, but importantly there is no macroscopic condensate. Following the protocols of Jochim and collaborators, we compute the characteristic temperature at which this peak disappears, thus providing a phase diagram for a quasi-condensation onset temperature in the polarized case. Additional information about $n_B(\mathbf{q})$ is reflected in the behavior of the density profiles when the trap is removed. We show how quasi-condensed bosons have a distinctive signature; they evolve relatively slowly under time of flight.

Ultracold Fermi gases are a valuable resource for learning about strongly correlated superfluids. Their utility comes from their tunability [1] which allows the dimensionality, band structure, interaction strength, and spin imbalance to be freely varied. With these various parameters one can, in principle, simulate a number of important condensed matter systems ranging from preformed pair and related effects in the high T_c cuprates [2–4] to intrinsic topological superfluids [5–7] and other exotic pairing states.

In this paper we focus on recent experiments [8, 9] on two-dimensional (2D) spin-imbalanced Fermi gases. These imbalance effects are believed [10] to have related effects in studies of color superconductivity and quark-gluon plasmas. In condensed matter systems, lower dimensional imbalanced superfluids are thought to be ideal for observing more exotic phases, such as the elusive LOFF state [11], or Berezinskii-Kosterlitz-Thouless (BKT) [12, 13] phase with algebraic order. At the heart of the present paper is the challenge of understanding the interplay between the dominant fluctuation effects, which destroy true long range order [14], and spin imbalance. The approach we use has been rather successful in addressing 2D low temperature quasi-condensation [15] in balanced Fermi gases.

In addition to addressing existing experiments, here we present predictions for future very low temperature experiments on these 2D gases. We follow the experimental procedures outlined in Refs. [16, 17] for the balanced case. Because of their relevance, we consider only trapped gases; here phase separation effects predominate. Importantly, our calculations find no true long range order. Nevertheless, as in Refs. [16, 17] we show how the pair-momentum distribution, $n_B(\mathbf{q})$ contains important information about the phenomenon of "quasi-condensation". Additional information is provided by studying how $n_B(\mathbf{q})$ affects the behavior of density profiles under time of flight analysis [9].

A central finding in this paper is that 2D spin-imbalanced systems in a trap exhibit a new form of phase separation involving non-condensed pairs. This is to be contrasted with three-dimensional gases [18, 19] where the phase separation is associated with a true condensate. The implications of this phase separation can be seen through a comparison with experiments [8] performed at moderate temperatures for the in-situ density profiles across the range of BCS to BEC. Because almost all the pairs reside in the central portion of the trap, this leads to a nearly balanced core, as observed in recent experiments [8, 9]. As one goes to larger radii, there are one (at low T) or two (at moderate T) additional shells. The outermost shell is to be associated with a Fermi gas of majority atoms. An intermediate shell (if it exists) is partially polarized and consists of broken pairs with majority and some minority atoms. Our calculations indicate a necessary but not sufficient condition to reach the low temperatures required for quasi-condensation is that a partially polarized intermediate shell will not be present. Instead, at these sufficiently low temperatures, there is an abrupt transition from a balanced core to a normal Fermi gas.

We stress that there is no unambiguous evidence for true BKT physics in these cold (balanced) Fermi gases. Even in solid state superconductors the situation is still somewhat controversial [20, 21]. The concept of quasi-condensation as we use it here derives exclusively from concrete experimental considerations. The pair momentum distribution, $n_B(\mathbf{q})$, exhibits a strong peak at low momentum which disappears somewhat abruptly at a fixed temperature. Below this temperature we say there is "quasi-condensation". This peak, confirmed in balanced gases [16, 17] can, moreover, be probed from the perspective of time of flight analysis [9]. Low momentum pairs in this distribution, which may be thought of as quasi-condensed, are relatively unchanged with varying time, as compared with the higher q pairs and the fermions.

It is important to note that the BKT physics of bind-

ing and unbinding of vortex pairs is not evident either in these experiments or in our theory. Following experiments then, we focus on the distribution $n_B(\mathbf{q})$ as a proxy representing aspects of this 2D superfluidity.

Theoretical literature on imbalanced 2D superfluids has focused either on the very low temperature region (both the ground state [22, 23] and Kosterlitz-Thouless regimes [24, 25]), on possible LOFF phases [26] and on the polaronic limit [27, 28] where the spin imbalance is extreme. Notable are Monte Carlo studies on square lattices which report [29] that the LOFF phase is the ground state. Additionally there are studies [30] of the effects of Gorkov-Melik-Barkhudarov corrections on the mean-field tri-critical transition temperature.

Thus, when considering the entire range of temperatures and polarizations there are rather few theoretical studies. Here we use a t-matrix scheme. We note that t-matrix approaches, which have addressed the 2D limit for the unpolarized case, [31–35] have the general advantage of including the effects of non-condensed pairs which are missing from the alternative [24, 25] path integral schemes of the BCS-BEC crossover. An appropriate t-matrix scheme must meet three important criteria. Within this scheme: (i) One should be able to analytically verify that in two dimensions $T_c = 0$ in homogeneous systems. (ii) There are no difficulties or unphysical features associated with including polarization effects. (iii) One should be able to incorporate trap effects while addressing both the special physics of two dimensionality and including polarization.

To address the first of these we quote from Ref. [4] where it is stated that if one searches "*for the T_c at which long-range order sets in, one obtains zero in accordance with the Mermin-Wagner theorem. In some sense this is an excellent check whether one has a good solution to the t-matrix equations: the correct solution should give $T_c = 0$ in 2D.*" As for the second point, we note that introducing polarization in the widely used Nozieres and Schmitt-Rink (NSR) [36] approach is known to lead to inconsistencies even in the 3D case [37, 38].

We summarize this literature discussion by noting that the present t-matrix scheme meets the three criteria listed above; in particular, it is possible here to compare with experiment because one can include both trap and polarization effects.

I. THEORETICAL FORMALISM

The theory used here is based on the BCS-Leggett [39] ground state now extended to include finite temperatures and generalized to include polarization effects [40–43]. The associated polarized ground state was studied in earlier work by other groups [22]. Moreover, for the case of 2D balanced gases there is a compatibility [15] with recent experimental studies [16, 17]. Here one treats the self energy of non-condensed pairs as having a broadened BCS form associated with a pseudogap $\Delta_{\rm pg}$ which we, henceforth call Δ. This model self energy avoids dealing with the full and more complicated t-matrix associated with BCS-Leggett theory. This approximation was introduced only after extensive numerical studies [44]. An alternative analysis [45], which presented physical implications without numerical details, has raised some concern about its adequacy. Nevertheless, given its simplicity, there is clearly value in using this "pseudogap approximation" to make progress in understanding recent experiments [8, 9].

Without showing the details, which have appeared in the recent literature [15], we present two coupled equations that define a self-consistent fluctuation theory:

$$\sum_{\mathbf{k}} \left[\frac{1 - f\left(E_{\mathbf{k}\uparrow}\right) - f\left(E_{\mathbf{k}\downarrow}\right)}{2E_{\mathbf{k}}} - \frac{1}{2\epsilon_{\mathbf{k}} + \epsilon_B} \right] = a_0 \mu_{\rm pair}, \quad (1)$$

$$\sum_{\mathbf{q}} b\left(\frac{\mathbf{q}^2}{2M_B} - \mu_{\rm pair} \right) = a_0 \Delta^2. \quad (2)$$

Here, the two-band Bogoliubov quasiparticle dispersion $E_{\mathbf{k}\sigma} = \sigma\, h + \sqrt{\xi_{\mathbf{k}}^2 + \Delta^2}$ ($\uparrow, \downarrow$ correspond to $\sigma = +1, -1$ respectively) is constructed from the bare fermions with excitation spectrum $\xi_{\mathbf{k}} = \epsilon_{\mathbf{k}} - \mu$ and pairing gap Δ. The fermions of mass m and momentum $\mathbf{k} = (k_x, k_y)$ have a single particle excitation spectrum $\epsilon_{\mathbf{k}} = \mathbf{k}^2/2m$, a fermionic chemical potential μ. An effective Zeeman field $h > 0$ shifts the energy of (majority) spin-up relative to the (minority) spin-down Fermi surfaces. We have also introduced the usual Bose and Fermi distribution functions $b(x)$ and $f(x)$, and included the two-particle binding energy ϵ_B [4] to regularize Eq. (1). Throughout this paper we set $\hbar = 1$.

The key physics in our system is captured by Eqs. (1)-(2), which reflect the natural equilibrium between fermionic quasiparticles and non-condensed pairs or bosons. Specifically, Eq. (2) introduces non-condensed bosonic degrees of freedom which have momentum $\mathbf{q}$, mass M_B, and chemical potential $\mu_{\rm pair}$. (M_B and the constant a_0 are calculated from an expansion of a t-matrix describing paired bosons. See the Supplemental Material in Ref. [15] for a precise definition.)

These fluctuations are not present in the strict mean-field theory of BCS; if one sets the pair chemical potential $\mu_{\rm pair}$ to zero, then Eq. (1) reduces to the usual mean-field equation for a polarized gas, specifying the gap parameter Δ. Including these fluctuations then allows one to solve for the two unknowns: Δ and $\mu_{\rm pair}$. The fermions are associated with the energy Δ needed to break apart pairs, and the non-condensed bosonic pairs have a self-consistently determined chemical potential $\mu_{\rm pair}$, which depends on the pairing gap Δ. Here the number density of pairs (bosonic number) is given by $n_B = a_0 \Delta^2$. The more non-condensed bosons which are present, the larger the pairing gap. That these bosonic degrees of freedom cannot condense (at finite T) in 2D leads to the absence of any finite temperature instability. We can think of these as the introduction of fluctuation effects.

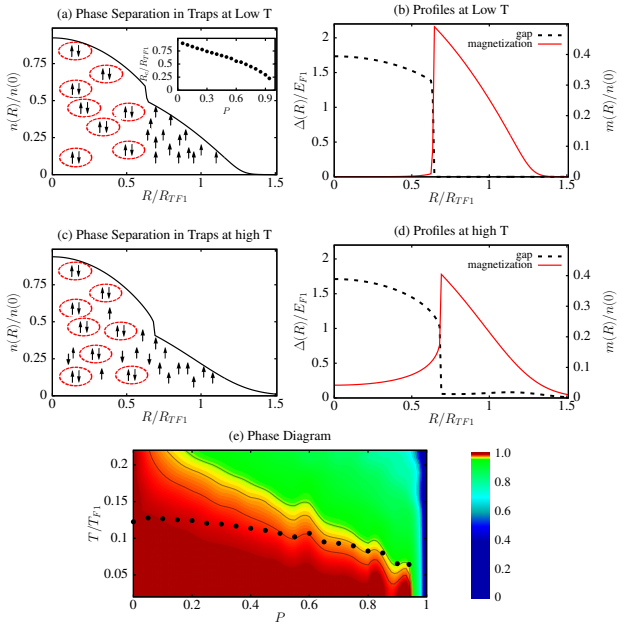

FIG. 1. This figure contrasts the nature of phase separation in a harmonic trap at low temperatures ((a) and (b)) where quasi-condensation occurs ($T/T_{F1} = 0.06$) and moderate temperatures ((c) and (d)) ($T/T_{F1} = 0.22$) more appropriate to experiments [8, 9]; the binding energy is fixed at $E_{F1}/\epsilon_B = 0.75$ and the total polarization $P = (N_\uparrow - N_\downarrow)/(N_\uparrow + N_\downarrow) = 0.5$. Black lines represent the local density $n(R)$ in (a) and (c), while in (b) and (d) the pairing gap $\Delta(R)$ is black (dashed) and the magnetization $m(R)$ is red (solid). Panel (a) shows the "two shell" structure: the core region, next to a fully polarized region, is occupied only by pairs. The radius at which the gap turns off abruptly at low T is indicated as an inset in (a). The density profile in panel (c) exhibits a "three shell" structure: the almost balanced core region is followed by a transition region that is partially polarized and the edge is fully polarized. Finally panel (e) presents a phase diagram where the color contours indicate the central balance ratio, $\tilde{p}(0) = n_\downarrow(0)/n_\uparrow(0)$, of minority to majority atoms at the trap center. The three contours mark values of 99%, 98%, and 97% for this ratio. The black dots mark the onset of quasi-condensation, as defined in Eq. (4).

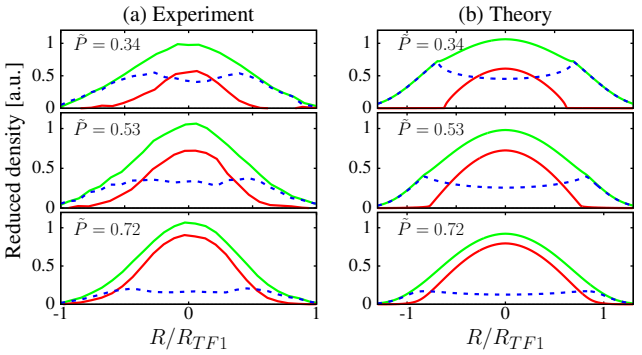

FIG. 2. Comparison of integrated column density profiles of (a) experiment [8] and (b) theory for a trapped system with $E_{F1}/\epsilon_B = 0.75$ and $T/T_{F1} = 0.22$. The green, red, and blue curves are the reduced densities (see [8] for definition) of the majority, minority, and magnetization (difference), respectively. The legend indicates the total balance ratio $\tilde{P} = N_\downarrow/N_\uparrow$. A transition to a nearly balanced core is seen in both theory and experiment.

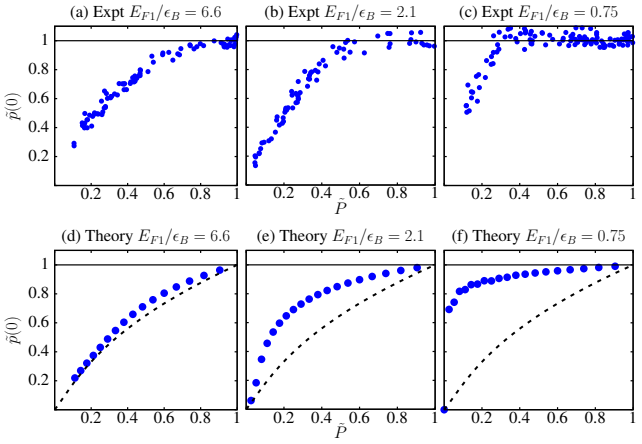

FIG. 3. Comparison of theoretical and experimentally measured [8] values of the central balance ratio $\tilde{p}(0) = n_\downarrow(0)/n_\uparrow(0)$. For theoretical results $T/T_{F1} = 0.22$. The dashed curves give the ideal Fermi gas limit ($\epsilon_B = 0$); the solid black curves are guides to the eye.

In experiments, the effective Zeeman field h and total chemical potential μ derive from a magnetization $m = n_\uparrow - n_\downarrow$ and number density $n = n_\uparrow + n_\downarrow$. Thus we set the fermionic chemical potentials using the number equation

$$n_\sigma = \frac{1}{2}\sum_{\mathbf{k}}\left[\left(1 + \frac{\xi_{\mathbf{k}}}{E_{\mathbf{k}}}\right) f\left(E_{\mathbf{k}\sigma}\right) + \left(1 - \frac{\xi_{\mathbf{k}}}{E_{\mathbf{k}}}\right) f\left(-E_{\mathbf{k}\bar{\sigma}}\right)\right] \tag{3}$$

for the number density of species $\sigma = -\bar{\sigma}$.

To account for the trapping potential, we apply the local density approximation (LDA) to a system with total atom number $N_\uparrow$ ($N_\downarrow$) of majority (minority) carrier. Here we replace $\mu \to \mu(R) \equiv \mu_0 - \frac{1}{2}m\omega^2 R^2$, and $\Delta \to \Delta(R)$, where μ_0, ω, and R represent the central fermionic chemical potential, the trap frequency, and position respectively. Derived quantities such as the magnetization $m(R)$, number density $n(R)$, and pair mass $M_B(R)$ gain local dependence. However, the effective Zeeman field is independent of position throughout the trap. Where relevant we express energy and local position in units of the majority spin Fermi energy, $E_{F1} = \omega\sqrt{2N_\uparrow}$, and Thomas-Fermi radius $R_{TF1} = \sqrt{2E_{F1}/m\omega^2}$ respectively; we take $\omega/E_{F1} = 1/40$ comparable to Ref. [8]. We note here that the numerical results are independent of the choice of ω/E_{F1}.

In what follows it will be convenient to define a total polarization $P = (N_\uparrow - N_\downarrow)/(N_\uparrow + N_\downarrow)$. To connect with recent experiments [8], we will also define a "balance ratio" $\tilde{p}(R) = n_\downarrow(R)/n_\uparrow(R)$, and similarly for a total balance ratio $\tilde{P} = N_\downarrow/N_\uparrow$.

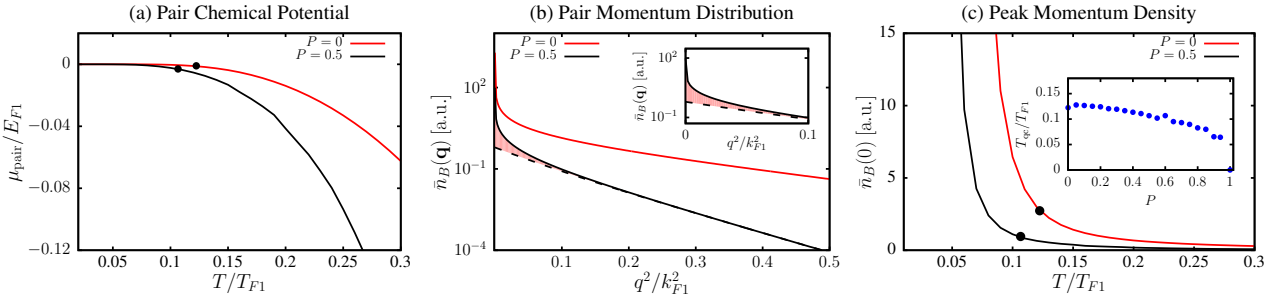

FIG. 4. Characteristics of quasi-condensation at a binding energy $E_{F1}/\epsilon_B = 0.75$. Pair chemical potential (a) for a polarized (black, $P = 0.5$) and unpolarized (red) Fermi gas. The small and non-zero size of $\mu_{\rm pair}$ reflects an exponential suppression at low temperatures [15]. (b) This leads to a low-momentum peak in the pair momentum distribution $\bar{n}_B(\mathbf{q})$ at low temperatures for these two different global polarizations. The shaded region indicates where the bosons are quasi-condensed and we refer to the non-shaded region as the thermal distribution $\bar{n}_{\rm th}(\mathbf{q})$, shown for $P = 0.5$ (see main text). The inset is an enlarged view of the case $P = 0.5$. (c) The dependence of the $\bar{n}_B(0)$ peak on temperature allows the extraction (dots) of $T_{\rm qc}$ in Eq. (4). The inset shows the dependence of $T_{\rm qc}$ on P.

II. NUMERICAL RESULTS

Figure 1 serves to clarify the concept of phase separation in a trapped 2D gas for both low ($T/T_{F1} = 0.06$) and moderate temperatures ($T/T_{F1} = 0.22$). The former are applicable to the quasi-condensation regime discussed below, while the latter are closer to the temperature range studied experimentally [8, 9]. We consider an intermediate binding energy $E_{F1}/\epsilon_B = 0.75$. The density profiles as a function of position in these two temperature regimes are plotted in panels (a) and (c), along with a cartoon illustration of the nature of the gas, as the radius changes. Panels (b) and (d) provide useful information on the gap profiles (black) and magnetization profiles (red). The radius at which the gap turns off abruptly at low T is indicated as an inset in (a).

At lower temperatures there is an abrupt boundary separating a fully paired state in the core (indicated by the paired spins in the cartoon) and a non-interacting fully polarized gas of majority spins (also represented in a cartoon fashion). We refer to these profiles as containing only "two shells": composite bosons at the core and majority fermions surrounding it. Importantly, one sees that the magnetization in Fig. 1(b) and the gap both change nearly discontinuously.

Although the number density profile in Fig. 1(c) behaves similarly to its low-T counterpart, one sees here (using information about the calculated gap, local polarization, and magnetization), that there are now "three shells" in the structure, as shown in the cartoon. The core region contains mostly non-condensed pairs with very little magnetization. As one goes away from the trap center, the local magnetization initally increases resulting in a middle shell. Finally, toward the edge of the trap where the magnetization drops, the gas is non-interacting ($\Delta(R) = 0$) and fully polarized. The presence of these multiple shells was emphasized in Ref. [9]. The major difference between two-shell and three-shell structures is the appreciable magnetization just inside the phase separation radius.

These calculations suggest that the magnetization versus position R serves as a kind of thermometry. In particular, that we are able to associate the lower-T behavior with the existence of a (quasi-)condensate, can be inferred from the phase diagram plotted in Fig. 1(e). Here the vertical and horizontal axes represent temperature T, and total polarization P, respectively. As indicated in the legend, the colors more precisely correspond to the ratio of minority to majority spins at the trap center. The three contours mark 99%, 98%, and 97% for the ratio. The black dots on the phase diagram show where we find pair (quasi-)condensation, as will be discussed below. It should be clear that this quasi-condensate essentially always appears in conjunction with our "two shell" profiles.

III. COMPARISON WITH EXPERIMENT

The general picture described above has implications which are directly relevant to recent experiments. We now present comparisons with experimental data [8]. In Fig. 2 we plot "column density" profiles for majority and minority components in the trap along with the difference profile (local magnetization), for three different values of the balance ratio $\tilde{P}$. (The total polarization increases as one goes upward on the three panels). In the calculations, we consider fixed moderate temperature $T/T_{F1} = 0.22$. The counterpart experimental data is plotted on the left along with theory curves on the right. That there is reasonable semi-quantitative agreement suggests that phase separation of a non-condensate, which was discussed in Fig. 1, is reflected in these actual experiments.

Indeed, there is a particularly interesting indicator of this form of phase separation. The ratios of minority to majority 2D densities at the trap center have been measured by Thomas and collaborators [8]. These experiments investigate the variation as one crosses from

more BCS to more BEC like behavior. They observe (see Fig. 3, top panels) the somewhat striking result that, away from the BCS regime, there is a rather abrupt transition from a balanced core to an unpaired phase at a critical polarization (which is presumably temperature dependent). The constancy of the data points indicates the very strong tendency to maintain maximal pairing until it is no longer possible. The abrupt drop occurs presumably because one has crossed the so-called $T^*(P)$ line. This temperature T^* marks the end-point of a normal state pairing gap, Δ, often called the pseudogap.

In Fig. 3 we present a comparison between theoretical and experimental results, plotting the central balance ratio $\tilde{p}(0)$ as a function of the total balance ratio $\tilde{P}$. In our theoretical analysis we fix the temperature for all panels at $T/T_{F1} = 0.22$. In the stronger pairing cases (with $E_{F1}/\epsilon_B = 0.75$ and $E_{F1}/\epsilon_B = 2.1$, as shown in the two panels to the right) the persistence of a balanced core for a range of total polarizations is observed. The theory curves are not quite as flat as in experiment. This might be explained if the theory temperatures are slightly higher than in experiment. There are also subtle but important effects [46] associated with special two dimensional features in the profile shapes, which are not captured in the present theory. Nevertheless, in both Fig. 3(b) and Fig. 3(c) the downward departure, as in experiment, is reasonably sudden.

These curves reflect simple changes in the trap profile; as $\tilde{P}$ increases, the boundary between balanced and imbalanced regions moves toward the trap center, (shown in the inset to Fig. 1(a)) while not affecting the magnetization at the precise "center". For smaller ϵ_B at finite T, the balanced core is narrower and the magnetization at the center also increases more rapidly as compared to larger ϵ_B. At sufficiently high P, for this temperature regime the system is driven normal and the profiles are those of an ideal Fermi gas.

IV. QUASI-CONDENSATION AT VERY LOW TEMPERATURES

We turn now to lower temperatures and to considerations of quasi-condensation following the concepts introduced in Ref. [9, 16]. The evidence from experiments [16, 17] on 2D spin-balanced Fermi gases suggests that the bosonic degrees of freedom (accessed by rapid magnetic field sweeps) exhibit strong $|\mathbf{q}| \to 0$ peaks in their momentum distribution, represented by a trap-average, denoted $\bar{n}_B(\mathbf{q})$, of $n_B(\mathbf{q}, \mathbf{R}) = b\left(\mathbf{q}^2/2M_B(R) - \mu_{\rm pair}(R)\right)$ appearing in Eq. (2). What is most significant [15] is that these peaks disappear rather abruptly at a particular temperature, $T_{\rm qc}$, which one associates with the onset of quasi-condensation.

Following the same analysis for a spin-imbalanced Fermi gas, in Fig. 4(a) we plot the pair chemical potential $\mu_{\rm pair}$ at the trap center for an unpolarized (in red) and a polarized gas (in black, $P = 0.5$). We find $\mu_{\rm pair}$ serves to determine the size of the peak structure in $\bar{n}_B(\mathbf{q})$ as can be seen from Eq. (2). In both the balanced and imbalanced cases, this pair chemical potential is found to be very small at low temperatures and strictly vanishes only in the ground state. This signifies a bosonic momentum distribution that is sharply peaked, but never acquires a macroscopic condensate at $T \neq 0$. Moreover, it is seen that the effects of spin imbalance are relatively minor, resulting in only a small quantitative shift in $\mu_{\rm pair}$ compared to the balanced case.

Figure 4(b) presents the counterpart plots of $\bar{n}_B(\mathbf{q})$ versus $\mathbf{q}$ where the two curves correspond to $P = 0$ in red and $P = 0.5$ in black. The latter is enlarged in the inset, where the peak in the momentum distribution at $\mathbf{q} = 0$ is evident. The temperature dependence of this peak is reflected in Fig. 4(c). The solid dots indicate the temperature, $T_{\rm qc}$, at which the pair chemical potential begins to deviate from effectively zero. Taking the deviation point as in Ref. [15] (which roughly corresponds to about a 1% shift from the background) yields

$$k_B T_{\rm qc} \approx \frac{\pi}{2.3} \frac{\hbar^2 n_B(T = T_{\rm qc})}{M_B(T = T_{\rm qc})}, \tag{4}$$

where we use the Bose number density $n_B(T = T_{\rm qc})$ and the pair mass $M_B(T = T_{\rm qc})$ at the trap center. The inset of Fig. 4(c) presents a plot of this quasi-condensation temperature as a function of total polarization. The effects of polarization on this temperature are relatively weak, presumably because of the phase separated and fully balanced spin core.

These same results are summarized by the black dots in Fig. 1(e) which presents a generalized phase diagram indicating the P, T parameters at which there is phase separation, as represented by the imbalance at the trap center. We note that the characteristic inner-core radius, which is plotted as an inset in Fig. 1(a), shows that for moderate polarizations the range in radii over which one has pairing (and therefore quasi-condensation) is restricted. This makes it difficult to perform the analysis that addresses power laws vs exponential fitting functions in the Fourier transform of $\bar{n}_B(\mathbf{q})$, which was identified [17] with $g_1(r)$. For the unpolarized case, such an analysis [15] further substantiated the identification of $T_{\rm qc}$ with the expression in Eq. (4).

A. Time-of-flight behavior

In this subsection, we discuss the time-of-flight behavior of two-dimensional polarized fermions, making a connection to recent experiments [9]. Of interest is the time of flight evolution of the bosonic contribution to the density profile. Figure 4(b) shows that the bosonic momentum distribution exhibits a pronounced low momentum peak, at sufficiently low temperatures in 2D. Importantly, this is what we associate with the concept of quasi-condensation. As the authors of Ref. [9] have

argued, one might learn about the degree of 2D condensation (or equivalently, the bosonic momentum distribution $n_B(\mathbf{q})$) by positing that these quasi-condensed bosons have a distinctive signature; they evolve relatively slowly under time of flight.

To probe this conjecture, here we study the time-dependece of the quasi-condensate defined as $n_{\rm qc}(\mathbf{q},\mathbf{R}) \equiv n_B(\mathbf{q},\mathbf{R}) - n_{\rm th}(\mathbf{q},\mathbf{R})$, where $n_{\rm th}(\mathbf{q},\mathbf{R})$ is the corresponding thermal fraction of the total density distribution (the trap average of which, $\bar{n}_{\rm th}(\mathbf{q})$, is shown as the non-shaded region in Fig. 4(b)) computed from the Boltzmann distribution with the same $M_B(R)$ and $\mu_{\rm pair}(R)$. This decomposition into components has appeared in Ref. [15, 16]. The time of flight behavior should also provide an indication of the quasi-condensation temperature, $T_{\rm qc}$. When temperatures are below this onset, one can expect that $n_{\rm qc}$ is mainly made up of small $\mathbf{q}$ bosons and, during the time-of-flight, the profile will not move significantly.

In the current LDA scheme, because the bosons do not directly interact, we are able to semi-classically compute the time dependence of $n_{\rm qc}$ as functions of R after the trap is released. If we define $\boldsymbol{\ell} \equiv \mathbf{R} - \mathbf{R}'$, then we have

$$n_{\rm qc}(\mathbf{R},t) = \int d^2\mathbf{q} d^2\mathbf{R}' n_{\rm qc}(\mathbf{q},\mathbf{R}') \delta^2\left(\frac{\mathbf{q}}{M_B(R')}t - \boldsymbol{\ell}\right), \tag{5}$$

where t is expansion time and we assume that the functional forms of the bosonic mass and pair chemical potential, $M_B(R)$ and $\mu_{\rm pair}(R)$, appearing in $n_{\rm qc}(\mathbf{q},\mathbf{R})$ remain the same for the short time scales considered in experiment; one presumes that t is on the order of the inverse trap frequency, ω^{-1}. From the above expression, it is straightforward to show that the total number of quasi-condensed bosons in a trap is independent of t:

$$\int d^2\mathbf{R} n_{\rm qc}(\mathbf{R},t) = \int d^2\mathbf{q} d^2\mathbf{R}' n_{\rm qc}(\mathbf{q},\mathbf{R}'). \tag{6}$$

In Fig. 5 we plot $n_{\rm qc}(\mathbf{R},t)$ at $t \neq 0$ and $t = 0$ for two different global polarizations. Important is the contrast between low and high temperatures, with the former plotted in the left hand panels and the latter on the right. Because the peaks in $n_B(\mathbf{q})$ are relatively sharper for the case $P = 0$, we consider a slightly longer characteristic time $t = 4/\omega$. For finite global polarization $P = 0.5$, the low momentum peak in Fig. 4(b) is not as pronounced; that is, there are fewer quasi-condensed bosons in the presence of polarization so for illustration purposes we chose a slightly shorter characteristic time $t = 1/\omega$. This allows us to illustrate a meaningful contrast in the time-of-flight behavior between low temperature $T = 0.06T_{F1}$ and high temperature $T = 0.22T_{F1}$. Note also that at $t = 0$, the magnitude of $n_{\rm qc}(\mathbf{R},t)$ at $T = 0.06T_{F1}$ is larger than that at $T = 0.22T_{F1}$, reflecting the fact that the non-thermal part decreases when temperature is increased.

From Figs. 5(a) and 5(b), which represent the $P = 0$ case, we find that at finite time the profiles move outward from the center, as one would expect. However, the first

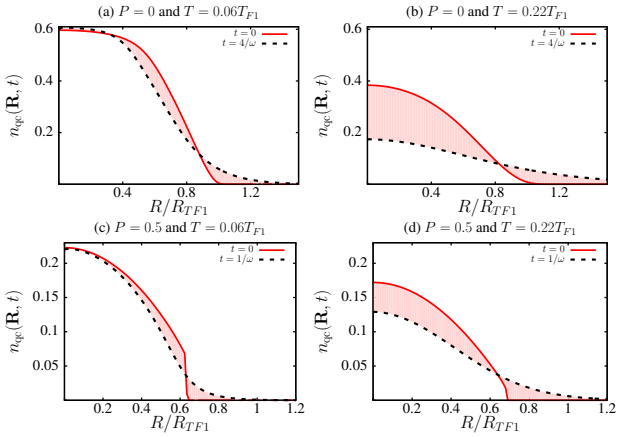

FIG. 5. Time-of-flight behavior of the quasi-condensate $n_{\rm qc}(\mathbf{R},t)$ (defined more precisely in the main text). The quantity $n_{\rm qc}$ at low and high temperature is plotted versus position for two different times, $t = 0$ and $t > 0$. In the first row, the global polarization $P = 0$ is considered while $P = 0.5$ for the second row. For these two different P, the bosonic profiles $n_{\rm qc}$ at both low and high temperatures move outward from the trap center with time. Notably, the profile varies more dramatically with time at high temperatures, as indicated by the shaded area.

of these figures shows relatively little change, reflecting the large number of quasi-condensed pairs at low temperatures. By contrast the profile at high T changes rather significantly, as indicated by the shaded area in Fig. 5. This can be attributed to the fact that in momentum space the bosonic density distribution is sharply peaked at low T and these low momemtum states move very little with time. In contrast, the non-thermal fraction at high T is not as sharply peaked as low T and the profile will move significantly.

For a finite global polarization $P = 0.5$, a similar behavior is observed; that is, $n_{\rm qc}$ at high T disperses much more quickly than low T as can be seen from the shaded region. These observations support the notion that one can learn about the momentum distribution of the quasi-condensate from time-of-flight studies. We are not in a position to argue that these studies establish the presence of a true macroscopically occupied $q = 0$ condensate, but rather that time-of-flight measurements provide useful constraints on the momentum distribution of paired states.

V. CONCLUSIONS

A goal of this paper has been to emphasize the distinction between the paired (normal state) and the lower temperature quasi-condensed phase of a 2D spin-imbalanced Fermi gas. We present a series of numerical results using a theory of the 2D polarized gas in a trap with variable temperature and polarization. Alternative theories such as those based on the Nozieres Schmitt-Rink [36] schemes

suffer from a shortcoming [37, 38] that polarization effects cannot be consistently accomodated, particularly near unitarity.

We show that low and moderate temperatures are associated with a balanced or nearly balanced core, but the nature of the related phase separation is somewhat distinctive, leading to more abrupt boundaries when quasi-condensation is present. Proving the existence or non-existence of true phase coherence would lead to a significant advance in the understanding of the physics of 2D Fermi gases. As in previous work [15–17] true superfluidity in 2D has not been established here or unambiguously identified in experiments. This will require future experimental probes related to coherence features, including interference measurements, or detection of the presence of collective modes in Bragg scattering.

Acknowledgments.— This work was supported by NSF-DMR-MRSEC 1420709. We thank J. Thomas for stimulating conversations and for sharing his data. We are grateful to W. Bakr and D. Mitra for useful discussions and information about their experiment.

[1] W. Ketterle and M. W. Zwierlein, in *Ultra-cold Fermi Gases*, edited by M. Inguscio, W. Ketterle, and C. Salomon (Italian physical society, 2007) p. 95.
[2] Q. J. Chen, J. Stajic, S. N. Tan, and K. Levin, Phys. Rep. **412**, 1 (2005).
[3] A. Perali, P. Pieri, G. C. Strinati, and C. Castellani, Phys. Rev. B **66**, 024510 (2002).
[4] V. M. Loktev, R. M. Quick, and S. G. Sharapov, Physics Reports **349**, 1 (2001).
[5] H. Zhai, Rep. Prog. Phys. **78**, 026001 (2015).
[6] C. Zhang, S. Tewari, R. M. Lutchyn, and S. Das Sarma, Phys. Rev. Lett. **101**, 160401 (2008).
[7] M. Iskin and A. L. Subaş ı, Phys. Rev. Lett. **107**, 050402 (2011).
[8] W. Ong, C. Cheng, I. Arakelyan, and J. E. Thomas, Phys. Rev. Lett. **114**, 110403 (2015).
[9] D. Mitra, P. Brown, P. Schauss, S. Kondov, and W. Bakr, "Phase separation and pair condensation in a spin-imbalanced 2d fermi gas," (2016), arXiv/1604.01479.
[10] E. Gubankova, A. Schmitt, and F. Wilczek, Phys. Rev. B **74**, 064505 (2006).
[11] R. Casalbuoni and G. Nardulli, Rev. Mod. Phys. **76**, 263 (2004).
[12] J. M. Kosterlitz and D. J. Thouless, J. Phys. C. Solid State **6**, 1181 (1973).
[13] V. Berezinskii, Sov. Phys. JETP **34**, 610 (1972).
[14] N. D. Mermin and H. Wagner, Phys. Rev. Lett. **17**, 1133 (1966).
[15] C.-T. Wu, B. M. Anderson, R. Boyack, and K. Levin, Phys. Rev. Lett. **115**, 240401 (2015).
[16] M. G. Ries, A. N. Wenz, G. Zürn, L. Bayha, I. Boettcher, D. Kedar, P. A. Murthy, M. Neidig, T. Lompe, and S. Jochim, Phys. Rev. Lett. **114**, 230401 (2015).
[17] P. A. Murthy, I. Boettcher, L. Bayha, M. Holzmann, D. Kedar, M. Neidig, M. G. Ries, A. N. Wenz, G. Zürn, and S. Jochim, Phys. Rev. Lett. **115**, 010401 (2015).
[18] G. B. Partridge, W. Li, R. I. Kamar, Y. A. Liao, and R. G. Hulet, Science **311**, 503 (2006).
[19] Y. Shin, M. W. Zwierlein, C. H. Schunck, A. Schirotzek, and W. Ketterle, Phys. Rev. Lett. **97**, 030401 (2006).
[20] J. Yong, T. R. Lemberger, L. Benfatto, K. Ilin, and M. Siegel, Phys. Rev. B **87**, 184505 (2013).
[21] S. T. Bramwell and P. C. W. Holdsworth, Phys. Rev. B **49**, 8811 (1994).
[22] L. He and P. Zhuang, Phys. Rev. A **78**, 033613 (2008).
[23] G. J. Conduit, P. H. Conlon, and B. D. Simons, Phys. Rev. A **77**, 053617 (2008).
[24] J. Tempere, S. N. Klimin, and J. T. Devreese, Phys. Rev. A **79**, 053637 (2009).
[25] S. N. Klimin, J. Tempere, J. T. Devreese, and B. Van Schaeybroeck, Phys. Rev. A **83**, 063636 (2011).
[26] D. E. Sheehy, Phys. Rev. A **92**, 053631 (2015).
[27] M. M. Parish, Phys. Rev. A **83**, 051603 (2011).
[28] M. M. Parish and J. Levinsen, Phys. Rev. A **87**, 033616 (2013).
[29] M. J. Wolak, B. Grémaud, R. T. Scalettar, and G. G. Batrouni, Phys. Rev. A **86**, 023630 (2012).
[30] M. A. Resende, A. L. Mota, R. L. S. Farias, and H. Caldas, Phys. Rev. A **86**, 033603 (2012).
[31] N. E. Bickers, D. J. Scalapino, and S. R. White, Phys. Rev. Lett. **62**, 961 (1989).
[32] F. Marsiglio, P. Pieri, A. Perali, F. Palestini, and G. C. Strinati, Phys. Rev. B **91**, 054509 (2015).
[33] M. Matsumoto, D. Inotani, and Y. Ohashi, (2015), arXiv:1507.05149.
[34] R. Watanabe, S. Tsuchiya, and Y. Ohashi, Phys. Rev. A **88**, 013637 (2013).
[35] M. Bauer, M. M. Parish, and T. Enss, Phys. Rev. Lett. **112**, 135302 (2014).
[36] P. Nozières and S. Schmitt-Rink, J. Low Temp. Phys. **59**, 195 (1985).
[37] P.-A. Pantel, D. Davesne, and M. Urban, Phys. Rev. A **90**, 053629 (2014).
[38] M. M. Parish, F. M. Marchetti, A. Lamacraft, and B. D. Simons, Nature Phys. **3**, 124 (2007).
[39] A. J. Leggett, in *Modern Trends in the Theory of Condensed Matter* (Springer-Verlag, Berlin, 1980) pp. 13–27.
[40] Y. He, C.-C. Chien, Q. Chen, and K. Levin, Phys. Rev. B **76**, 224516 (2007).
[41] C.-C. Chien, Q. J. Chen, Y. He, and K. Levin, Phys. Rev. A **74**, 021602(R) (2006).
[42] C.-C. Chien, Q. J. Chen, Y. He, and K. Levin, Phys. Rev. Lett. **97**, 090402 (2006).
[43] Q. Chen, Y. He, C.-C. Chien, and K. Levin, Phys. Rev. B **75**, 014521 (2007).
[44] J. Maly, B. Jankó, and K. Levin, Physica C **321**, 113 (1999).
[45] H. Hu, X.-J. Liu, and P. D. Drummond, Phys. Rev. A **77**, 061605(R) (2008).
[46] A. A. Orel, P. Dyke, M. Delehaye, C. J. Vale, and H. Hu, New Journal of Physics **13**, 113032 (2011).